

# Dual-loop control strategy applied to PV/battery-based islanded DC microgrids for swarm electrification of developing regions

eISSN 2051-3305

Received on 26th October 2018

Accepted on 09th January 2019

E-First on 27th June 2019

doi: 10.1049/joe.2018.9274

www.ietdl.org

Mashood Nasir<sup>1,2</sup> ✉, Hassan Abbas Khan<sup>1</sup>, Kamran Ali Khan Niazi<sup>2</sup>, Zheming Jin<sup>2</sup>, Josep M. Guerrero<sup>2</sup>

<sup>1</sup>SBASSE, Lahore University of Management Sciences, Lahore, Pakistan

<sup>2</sup>Department of Energy Technology, Aalborg University, Aalborg, Denmark

✉ E-mail: mashood.nasir@lums.edu.pk

**Abstract:** In this work, a dual-loop control strategy is applied to a highly distributed architecture of photovoltaic (PV)/battery-based DC microgrid, suitable for swarm electrification of developing regions. Typically, in such schemes, resource sharing among the spatially dispersed PV generation and battery storage resources is enabled via communication-based control methodologies, which adds cost and complexity to the overall system. Alternately, a communication-less and decentralised control methodology is proposed which utilises inner loop current control and outer loop voltage droop ( $V-I$  droop) control for the coordinated resource sharing among the distributed resources. Various scenarios of power sharing among the contributing households are evaluated and the efficacy of the proposed control scheme is validated through simulations on MATLAB/Simulink. Results show that the proposed decentralised control strategy is capable of ensuring stable and coordinated operation without any dedicated layer of communication among the dispersed generation/storage resources.

## 1 Introduction

Access to electricity and its consumption rates are the key factors for the assessment of socio-economic status of any community [1]. Reliable access to electricity is extremely crucial for human well-being and can contribute for better health, employment, agriculture and education opportunities. On the contrary, unavailability of electricity hampers the basic human rights including access to clean drinking water, proper lighting, and sustainable employment opportunities, therefore, declines the socio-economic status and tends to enhance the poverty [2]. According to International Energy Agency, around 1.1 billion people, i.e. 14% of global population are living without access to electricity [3]. The residents of these emerging regions have to largely rely on unhealthy resources like kerosene oil, even for lightning, which has many adverse effects on individuals as well as environment [4, 5]. Therefore, there is a world-wide focus on the electrification of these developing regions to attain the socio-economic benefits with the availability of electricity.

Photovoltaic (PV)/battery-based islanded DC microgrids are becoming very popular for the off-grid electrification of these developing regions due to green nature of PV operation, higher efficiency of DC distribution and lower costs associated with the distributed generation [6–8]. All the existing deployments use either centralised architecture (PV generation and battery storage at a centralised location) or distributed architecture (either generation or storage or both are spatially distributed). Centralised architectures are relatively simpler from installation, control, operation and maintenance prospective, however, they lack modularity and significant distribution losses are associated with their delivery of energy from generation end to utilisation end [9, 10]. Moreover, these architectures need centralised planning at the very outset; therefore, require relatively higher up-front cost for the system installation. Prominent practical installations are micro-solar plants in Chhattisgarh, Sunderbans and Lakshadweep in India [11, 12]. Mera Gao Power in Uttar Pradesh, India and the Jabula project in Cape Town, South Africa are other successful models of electrification via PV/battery-based islanded DC micro-grids [13, 14].

Distributed architectures can be further classified as partially or highly distributed architectures, based upon the distribution of PV generation and battery storage resources. Distributed architectures are generally more scalable and have relatively lower distribution

losses in comparison to centralised architectures [15–17]. Their modular nature imparts scalability to the overall microgrid structure, thereby centralised planning and upfront installation of resources is not mandatory for these distributed architectures. Rather, in such topologies, multiple household-level energy systems are interconnected to formulate a microgrid, where each household may operate independently along with the provisions of sharing resources with the neighbouring households. Such a community developed swarm of energy is organically scalable and capable to extract the benefit of usage diversity at a village scale [18]. However, they require sophisticated control techniques involving communication among the distributed resources for their stable and coordinated operation. The involvement of dedicated communication resources will not only add to the cost of the system but will also enhance the complexity of operation. From the perspective of rural electrification, such a complex and cost prohibitive solution is generally considered unviable for wide-scale adaption.

Various methodologies for the communication-less control of DC microgrids have been presented in the literature. Nasir *et al.* [16] presented a hysteresis-based voltage droop algorithm that adjusts the duty cycle of interfacing converters for stable operation of distributed microgrid. However, it does not consider the coordinated resource sharing in the microgrid structure. Therefore, during power-sharing mode, every household supplies or receives a constant amount of power irrespective of its own resource availability.

The dual-loop adaptive droop control scheme presented by Lu *et al.* [19] considers the partial coordination of distributed resources such that it considers power sharing proportional to the battery state of charge (SOC) index during power supply mode (battery discharge mode), but it does not consider power sharing in proportional to the SOC index during charging mode of the battery. Thereby all discharged batteries will get charge at the same rate irrespective of their resource deficiency. Also, the proposed scheme causes excessive distribution losses for unwanted SOC balancing and undesired charging/discharging of batteries in various households.

Alternatively, Nasir *et al.* [20] presented a fully coordinated adaptive droop scheme that considers resource sharing in proportional to SOC index for both charging and discharging modes. The proposed scheme employs an adaptive  $I-V$  droop

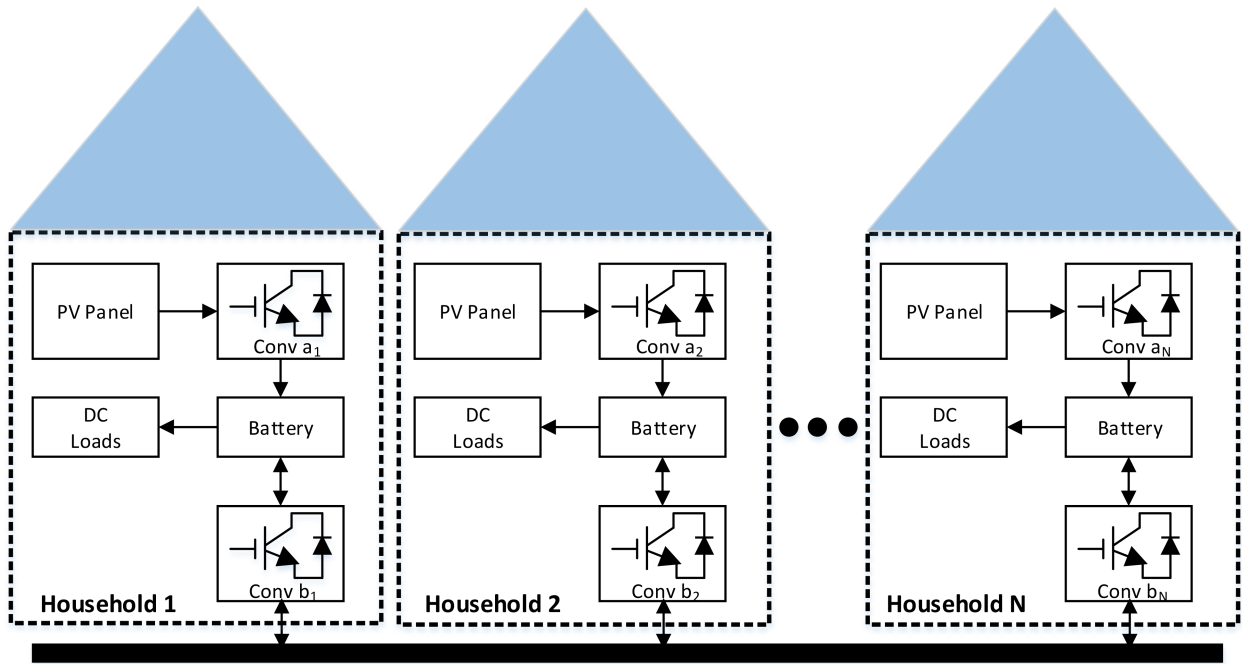


Fig. 1 Microgrid architecture as interconnection of  $N$  households

method which has superior transient performance in comparison to  $V-I$  droop method. However, the stability margins for  $I-V$  droop control are relatively smaller in comparison to  $V-I$  droop control, therefore, it may be subjected to instability due to the involvement of multiple constant power loads in the microgrid structure [21, 22].

In order to rectify these stability limitations and enable communication-less resource sharing in a coordinated manner, an adaptive dual-loop control strategy has been presented in this work. The proposed scheme is decentralised in nature and employs  $V-I$  droop control for enhanced stability margins. Rather than having a fixed slope for  $V-I$  droop, it has been configured as a function of SOC index of the battery for an individual household. Therefore, in case of power sharing, each house supply power in accordance to its resource availability and demand power in accordance with its resource deficiency as demonstrated by the results.

The rest of the paper is organised as follows. Section 2 highlights the structure of the highly distributed PV/battery-based DC microgrid and its individual components. Section 3 presents the dual-loop control strategy and various modes of operation for the interfacing converter. Section 4 presents the results for various possible power-sharing scenarios. Based on the results, conclusions are drawn in Section 5.

## 2 Distributed architecture of DC microgrid

Distributed generation and distributed architecture of PV/battery-based DC microgrid is shown in Fig. 1 [16, 20]. Each individual household has its own PV generation, battery storage and DC loads. Each household has two converters, where  $Conv a_i$  is responsible for optimal power extraction from PV panels and  $Conv b_i$  is responsible for bidirectional exchange of power between multiple households through DC bus. Each house can work independently as well as can share its resources with the neighbouring households. The resource sharing feature is enabled via proposed adaptive dual-loop control (inner current and outer voltage loop) of bi-directional converter and is detailed in the next section.

## 3 Adaptive control scheme

In order to interconnect multiple households without any physical communication layer among the dispersed resources, an adaptive control scheme is used for each bidirectional converter  $Conv b_i$ . Based on localised measurements of bus voltage  $V_o$  and battery

SOC converter may shift its mode of operation between (i) current controlled charging mode, (ii) current controlled discharging mode and (iii) dual-loop adaptive  $V-I$  droop mode. In each of these three modes, a current reference  $I_{ref}$  is generated as governed by (2)–(4). The inner loop proportional–integral (PI) current controller then generates the duty cycle  $D$  such that the desired current reference is achieved and battery is charged or discharged at the desired value of current

$$D = K_{p,i}(I_{ref} - I_{in}) + K_{i,i} \int_0^t (I_{ref} - I_{in}) dt \quad (1)$$

where  $K_{p,i}$  and  $K_{i,i}$  are the proportional and integral constants for inner current loop PI controller and  $I_{in}$  is the inductor current of the bi-directional converter at which battery is charged or discharged. Thus, by controlling the current sharing of each individual household based on the adaptive control strategy, a decentralised control ensuring stable and coordinated operation of the microgrid is achieved.

### 3.1 Current controlled charging mode

SOC index of the battery serves as an indicator of the resource availability in an individual household. When SOC falls below minimum threshold, i.e.  $SOC < SOC_{min}$ , its bi-directional converter switches in current controlled charging mode (CCCM). The current reference is generated based on the extent of resource deficiency such that it demands rated current  $I_{rated}$  when it is away from  $SOC_{min}$  and its current demand decreases as its SOC reaches to  $SOC_{min}$ . The PI controller then generates the duty cycle such that the desired current reference is achieved and battery is charged at the desired value of current governed by

$$I_{ref} = I_{rated} \left( \frac{SOC}{SOC_{min}} - 1 \right) \quad (2)$$

### 3.2 Dual-loop adaptive voltage droop control ( $V-I$ ) mode

In intermediate range of SOC, i.e.  $SOC_{min} \leq SOC \leq SOC_{max}$  each household has sufficient resource availability, therefore, it can either supply or demand power based on the requirements of neighbouring households. DC bus voltage  $V_o$  serves as an indicator of the requirements of neighbouring households. A value of  $V_o$  below the reference voltage  $V_{ref}$  indicates that one or more

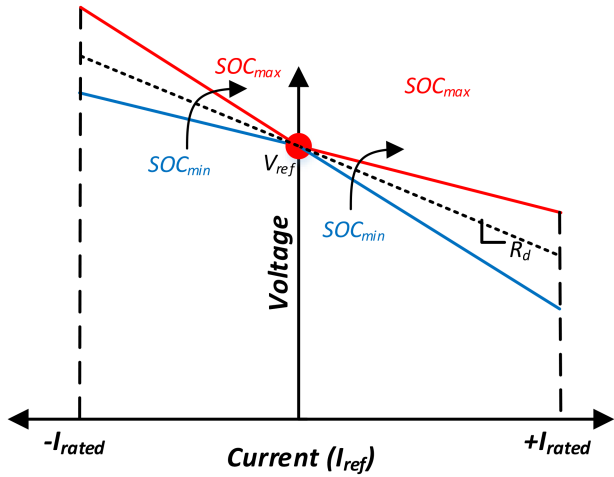


Fig. 2  $V$ - $I$  droop variations as a function of SOC

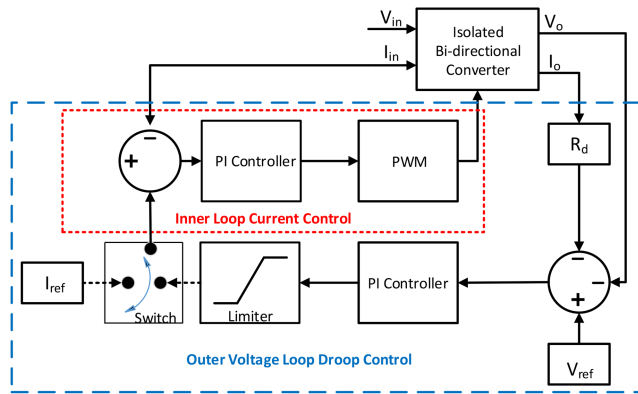


Fig. 3 Adaptive control scheme of the bidirectional converter

neighbouring houses in the microgrid structure are deficient in resources and they need to be charged. At this point, the households having higher resource availability, i.e. having higher SOC index should supply more power in comparison to those households which have relatively lower resource availability. This coordination is ensured through a modified discharging droop  $R_{dis}$  given by (3), whose visual depiction is also shown in Fig. 2.

$$R_{dis} = R_d \left[ 1 - 0.5 \left( \frac{SOC - SOC_{min}}{SOC_{max} - SOC_{min}} \right) \right] \quad (3)$$

$R_{dis}$  ensures that virtual droop impedance  $R_d$  which is generally considered constant in a conventional  $V$ - $I$  droop is decreasing here in a linear fashion from  $R_d$  to  $0.5R_d$  when SOC varies from  $SOC_{min}$  to  $SOC_{max}$ . Based on this varying droop function  $R_{dis}$ , an outer voltage droop loop generates reference for an inner loop current control as shown in Fig. 3 and given by

$$I_{ref} = K_{p,v}(V_{ref} - V_o - I_o R_{dis}) + K_{i,v}(V_{ref} - V_o - I_o R_{dis}) \quad (4)$$

where  $K_{p,v}$  and  $K_{i,v}$  are the proportional and integral constants for outer voltage loop PI controller and  $I_o$  is the output current of the bi-directional converter towards DC bus.

Similarly,  $V_o$  above the reference voltage  $V_{ref}$  indicates that one or more neighbouring houses are already saturated and they need to be discharged. Therefore, in this situation the households having lower resource availability, i.e. having lower SOC index should receive more power in comparison to those households which have relatively higher resource availability. This coordination is ensured through a modified charging droop  $R_{ch}$  given by (5), whose visual depiction is also shown in Fig. 2

$$R_{ch} = 0.5R_d \left[ 1 + \left( \frac{SOC - SOC_{min}}{SOC_{max} - SOC_{min}} \right) \right] \quad (5)$$

$R_{dis}$  ensures that virtual droop impedance  $R_d$  which is generally considered constant in a conventional  $V$ - $I$  droop is increasing here in a linear fashion from  $0.5R_d$  to  $R_d$  when SOC varies from  $SOC_{min}$  to  $SOC_{max}$ . Based on this varying droop function  $R_{ch}$ , an outer voltage droop loop generates reference for an inner loop current control as shown in Fig. 3 and given by

$$I_{ref} = K_{p,v}(V_{ref} - V_o - I_o R_{dis}) + K_{i,v}(V_{ref} - V_o - I_o R_{dis}) \quad (6)$$

where  $K_{p,v}$  and  $K_{i,v}$  are the proportional and integral constants for outer voltage loop PI controller and  $I_o$  is the input current of the bi-directional converter from DC bus.

Fig. 2 shows the variations of  $V$ - $I$  droop as a function of SOC. It can be seen that for positive values of current  $I_{ref}$ , i.e. when an individual household is supplying power, moving from  $SOC_{min}$  to  $SOC_{max}$  decreases the slope of  $V$ - $I$  curve and therefore, household with higher value of SOC supply more power in comparison to household having lower value of SOC. Similarly, for negative values of current  $I_{ref}$ , i.e. when an individual household is receiving power, moving from  $SOC_{min}$  to  $SOC_{max}$  increases the slope of  $V$ - $I$  curve and therefore, household with lower value of SOC receives more power in comparison to household having higher value of SOC and vice versa.

### 3.3 Current controlled discharging mode

When SOC of the battery in an individual household increases above maximum threshold due to higher incident solar irradiance and associated PV power generation, i.e.  $SOC > SOC_{max}$ , its bi-directional converter switches in current controlled discharging mode (CCDM). The current reference is generated based on the extent of resource saturation such that it supplies rated current  $I_{rated}$  when it is away from  $SOC_{max}$  and its current supply decreases as its SOC reaches to  $SOC_{max}$ . The PI controller then generates the duty cycle such that the desired current reference is achieved and battery is discharged at the desired value of current governed by

$$I_{ref} = I_{rated} \left( \frac{SOC_i - SOC_{max}}{100 - SOC_{max}} \right) \quad (7)$$

## 4 Case study, results and discussions

For the validation of the proposed control scheme, simulations are carried out in MATLAB/Simulink using physical models of the converters. Simulations are carried out on MATLAB/Simulink using physical models of the converters and control schematic shown in Figs. 2 and 3. Various parameters for simulation are also shown in Table 1.

The droop value  $R_d$  is selected according to the converter ratings and adjusted such that voltage of the microgrid is in between the allowable range for its full range of operation. Similarly, integral and proportional parameters for current loop and voltage loop controllers are chosen based on the closed-loop stability of the proposed scheme.

### 4.1 One house is in CCCM and remaining houses are in $V$ - $I$ droop mode

In this scenario, battery of house 1 is assumed below minimum threshold of SOC, i.e.  $SOC_1 = 10\%$ , while the batteries of the other three households are assumed within the specified maximum and minimum thresholds of SOC, i.e.  $SOC_2 = 35\%$ ,  $SOC_3 = 55\%$ ,  $SOC_4 = 75\%$ . The results of current sharing through the proposed decentralised control scheme are shown in Fig. 4. From Fig. 4, it can be seen that house 1 is demanding power in proportion to its resource deficiency as governed by (2), while houses 2, 3 and 4 are supplying power in proportion to their resource availability such that house 4 having highest resource availability (SOC index) is supplying highest amount of current and house 2 is supplying lowest value of current for charging the battery of house 1.

**Table 1** Parameters of simulated case study

Description of the parameter	Value
no. of nanogrids/households	4
input capacitance of each $Conv b_i$	220 $\mu$ F
inductance of each $Conv b_i$	2.1 mH
DC bus capacitance	10 mF
switching frequency for $Conv b_i$	10 kHz
battery capacity for each household	2400 Wh
rated charging current for the battery	10 A
rated voltage of each battery	24 V
maximum threshold of battery SOC	80%
minimum threshold of battery SOC	30%
reference voltage for DC bus	48 V
initial voltage of DC bus	24 V
droop coefficient for each $Conv b_i$	0.23 $\Omega$
parameters of current loop controller	0.33, 15
parameters of voltage loop controller	1.75, 10

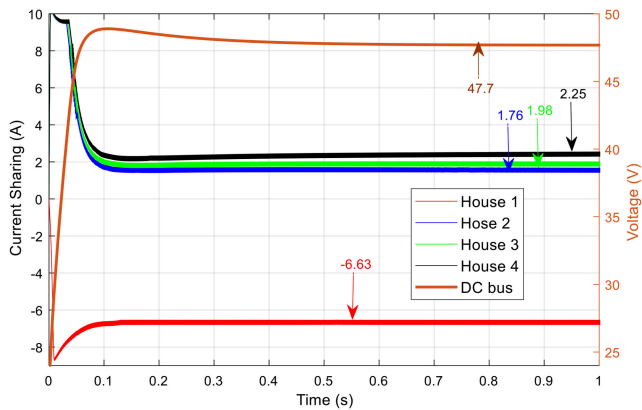


**Fig. 4** Simulation results for current sharing and DC bus voltage in case 1

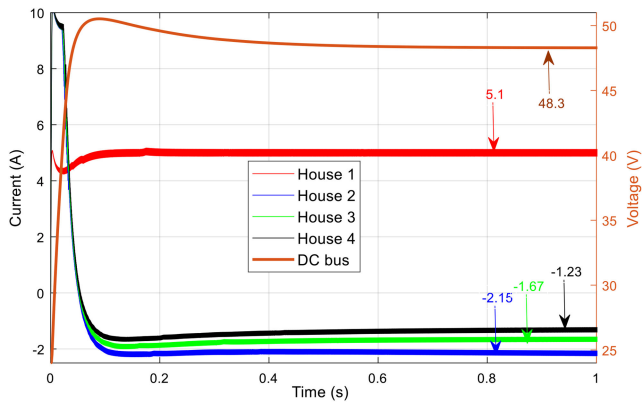


**Fig. 5** Simulation results for current sharing and DC bus voltage in case 2

**4.2 One house is in CCDM and remaining houses are in V-I droop mode**

In this scenario, battery of house 1 is assumed above maximum threshold of SOC, i.e.  $SOC_1 = 90\%$ , while the batteries of the other three households are assumed within the specified maximum and minimum thresholds of SOC, i.e.  $SOC_2 = 35\%$ ,  $SOC_3 = 55\%$ ,  $SOC_4 = 75\%$ . The results of current sharing through the proposed decentralised control scheme are shown in Fig. 5. From Fig. 5, it can be seen that house 1 is supplying power in proportion to its resource saturation as governed by (7), while houses 2, 3 and 4 are absorbing power in proportion to their resource deficiency such that house 2 having lowest resource availability (SOC index) is receiving highest amount of current and house 4 is receiving lowest value of current for charging their batteries from house 1.

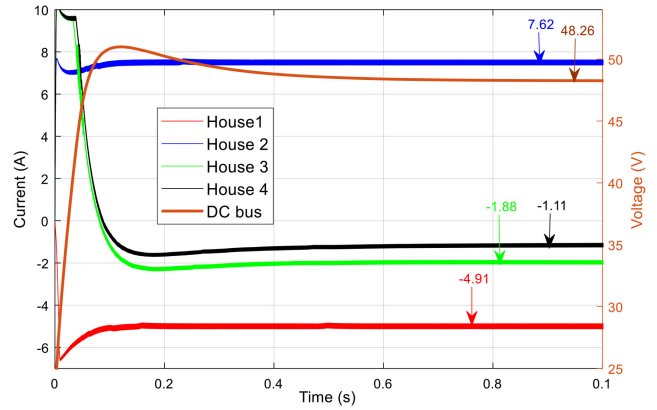


**Fig. 6** Simulation results for current sharing and DC bus voltage in case 3

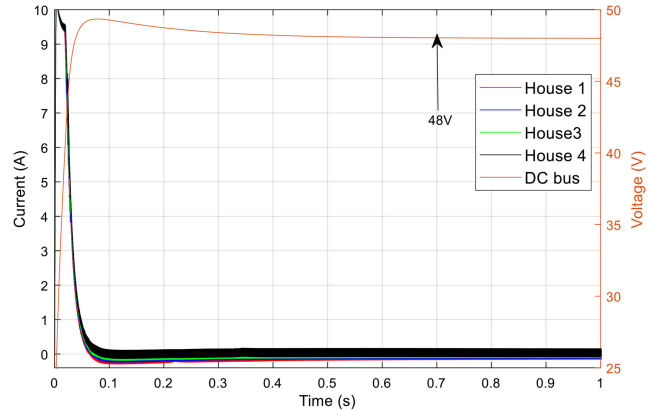


**Fig. 7** Simulation results for current sharing and DC bus voltage in case 4

**4.3 One house is in CCCM, one house in CCDM and remaining houses are in V-I droop mode**

In this scenario, battery of house 1 is assumed below minimum threshold of SOC, i.e.  $SOC_1 = 15\%$ , battery of house 2 is assumed above minimum threshold of SOC, i.e.  $SOC_2 = 95\%$ , while the batteries of the other two households are assumed within the specified maximum and minimum thresholds of SOC, i.e.  $SOC_3 = 55\%$ ,  $SOC_4 = 75\%$ . The results of current sharing through the proposed decentralised control scheme are shown in Fig. 6. From Fig. 6, it can be seen that house 1 is demanding power in proportion to its resource deficiency as governed by (2), house 2 is supplying power in proportion to its resource saturation as governed by (7), while houses 3 and 4 will supply/demand power in accordance to net current supplied at DC bus and its resulting voltage. Since in this scenario net current supplied by house 2 is higher than the current absorbed by house 1, therefore, net voltage of DC bus is higher than  $V_{ref}$ , as a result of which houses 3 and 4 are absorbing power in accordance to their resource deficiency such that household 2 being at lower SOC is being charged at relatively higher current in comparison to household 3 as shown in Fig. 6.

**4.4 All four houses are in V-I droop mode**

In this scenario, all four houses are assumed within the maximum and minimum threshold range of SOC. Results of current sharing and dc bus voltage are shown in Fig. 7. Since all the houses are self-sufficient, and are operating in V-I droop mode, voltage is stable at  $V_{ref}$  and there is no net power flow from one household to other via DC bus. In an optimally sized DC microgrid [23], households will be operating in this mode for most of the times, therefore, distribution losses will be minimum from generation end to utilisation end. This reduction in losses is otherwise not possible with the SOC balancing-based methodology presented in [19].

## 5 Conclusion

Distributed architectures of PV/battery-based islanded DC microgrids are generally more suitable for swarm electrification of developing regions provided they have a decentralised control strategy. In this work, such an adaptive control scheme using dual-loop voltage droop ( $V-I$ ) is presented and its validity is demonstrated with simulations results.  $V-I$  droop ensures higher stability margins, while SOC-based variations in droop enable coordinated resource sharing without dedicated communication resources. Therefore, distributed architecture with the proposed adaptive control scheme combines the advantage of both of the existing architectures, i.e. (i) lower distribution losses, (ii) scalability and modularity, (iii) communication-less coordinated control and (iv) stability over wide range of operation and is deemed highly suitable for future rural electrification deployments.

## 6 References

- [1] Bergasse, E., Paczynski, W., Dabrowski, M., *et al.* 'The relationship between energy and socio-economic development in the Southern and Eastern Mediterranean', 2013
- [2] Peters, J., Sievert, M.: 'Impacts of rural electrification revisited – the African context', *J. Dev. Effect.*, 2016, **8**, pp. 327–345
- [3] World Energy Outlook (WEO): 'Electricity access database', 2017. Available at [https://www.iea.org/publications/freepublications/publication/WEO2017SpecialReport\\_EnergyAccessOutlook.pdf](https://www.iea.org/publications/freepublications/publication/WEO2017SpecialReport_EnergyAccessOutlook.pdf)
- [4] González-Eguino, M.: 'Energy poverty: an overview', *Renew. Sust. Energy Rev.*, 2015, **47**, pp. 377–385
- [5] Lam, N.L., Smith, K.R., Gauthier, A., *et al.* 'Kerosene: a review of household uses and their hazards in low-and middle-income countries', *J. Toxicol. Environ. Health, B*, 2012, **15**, pp. 396–432
- [6] Schnitzer, D., Lounsbury, D.S., Carvallo, J.P., *et al.* 'Microgrids for rural electrification: a critical review of best practices based on seven case studies' (United Nations Foundation, Berkeley, CA, USA, 2014)
- [7] Justo, J.J., Mwasilu, F., Lee, J., *et al.* 'AC-microgrids versus DC-microgrids with distributed energy resources: a review', *Renew. Sust. Energy Rev.*, 2013, **24**, pp. 387–405
- [8] He, G., Victor, D.G.: 'Experiences and lessons from China's success in providing electricity for all', *Resour. Conserv. Recycl.*, 2017, **122**, pp. 335–338
- [9] Nasir, M., Zaffar, N.A., Khan, H.A.: 'Analysis on central and distributed architectures of solar powered DC microgrids'. 2016 Clemson University Power Systems Conf. (PSC), Clemson, SC, USA, 2016, pp. 1–6
- [10] Hamza, M., Shehroz, M., Fazal, S., *et al.* 'Design and analysis of solar PV based low-power low-voltage DC microgrid architectures for rural electrification'. 2017 IEEE Power & Energy Society General Meeting, Chicago, IL, USA, 2017, pp. 1–5
- [11] Mishra, S., Ray, O.: 'Advances in nanogrid technology and its integration into rural electrification in India'. 2014 Int. Power Electronics Conf. (IPEC-Hiroshima 2014-ECCE-ASIA), Hiroshima, Japan, 2014, pp. 2707–2713
- [12] Palit, D., Sarangi, G.K., Krithika, P.: 'Energising rural India using distributed generation: the case of solar mini-grids in Chhattisgarh state, India', in 'Mini-grids for rural electrification of developing countries' (Springer, New York, NY, USA, 2014), pp. 313–342
- [13] Urpelainen, J.: 'Energy poverty and perceptions of solar power in marginalized communities: survey evidence from Uttar Pradesh, India', *Renew. Energy*, 2016, **85**, pp. 534–539
- [14] Jabula Project, Zonk Energy serving off-grid communities with renewable energy. Available at <http://www.zonkeenergy.com/JabulaProject.php>
- [15] Inam, W., Strawser, D., Afridi, K.K., *et al.* 'Architecture and system analysis of microgrids with peer-to-peer electricity sharing to create a marketplace which enables energy access'. 2015 9th Int. Conf. Power Electronics and ECCE Asia (ICPE-ECCE Asia), Seoul, South Korea, 2015, pp. 464–469
- [16] Nasir, M., Khan, H.A., Hussain, A., *et al.* 'Solar PV-based scalable DC microgrid for rural electrification in developing regions', *IEEE Trans. Sustain. Energy*, 2018, **9**, pp. 390–399
- [17] Madduri, P.A., Poon, J., Rosa, J., *et al.* 'Scalable DC microgrids for rural electrification in emerging regions', *IEEE J. Emerging Sel. Topics Power Electron.*, 2016, **4**, pp. 1195–1205
- [18] Groh, S., Philipp, D., Lasch, B.E., *et al.* 'Swarm electrification-suggesting a paradigm change through building microgrids bottom-up'. 2014 3rd Int. Conf. Developments in Renewable Energy Technology (ICDRET), Dhaka, Bangladesh, 2014, pp. 1–2
- [19] Lu, X., Sun, K., Guerrero, J.M., *et al.* 'State-of-charge balance using adaptive droop control for distributed energy storage systems in DC microgrid applications', *IEEE Trans. Ind. Electron.*, 2014, **61**, pp. 2804–2815
- [20] Nasir, M., Jin, Z., Khan, H., *et al.* 'A decentralized control architecture applied to DC nanogrid clusters for rural electrification in developing regions', *IEEE Trans. Power Electron.*, 2018, **34**, (2), pp. 1773–1785, DOI: 10.1109/TPEL.2018.2828538
- [21] Gao, F., Bozhko, S., Costabeber, A., *et al.* 'Comparative stability analysis of droop control approaches in voltage-source-converter-based DC microgrids', *IEEE Trans. Power Electron.*, 2017, **32**, pp. 2395–2415
- [22] Jin, Z., Meng, L., Guerrero, J.M.: 'Comparative admittance-based analysis for different droop control approaches in DC microgrids'. 2017 IEEE Second Int. Conf. DC Microgrids (ICDCM), Nuremberg, Germany, 2017, pp. 515–522
- [23] Nasir, M., Iqbal, S., Khan, H.A.: 'Optimal planning and design of low-voltage low-power solar DC microgrids', *IEEE Trans. Power Syst.*, 2018, **33**, (3), pp. 2919–2928